Function of Cytochrome P450 *CYP72A1182* in Metabolic Herbicide Resistance Evolution in *Amaranthus palmeri* Populations

Running title: CYP72A1182* is Involved in Herbicide Resistance Evolution in *Amaranthus palmeri

Carlos Alberto Gonsiorkiewicz Rigon[1], Anita Küpper[2], Crystal Sparks[1], Jacob Montgomery[1], Falco Peter[2], Simon Schepp[2], Alejandro Perez-Jones[3], Patrick J. Tranel[4], Roland Beffa[5], Franck E. Dayan[1], Todd A. Gaines[1]

[1] Colorado State University, Department of Agricultural Biology, Fort Collins, CO 80523, USA. carlos.rigon@colostate.edu; crystal.sparks@colostate.edu; jake.montgomery@colostate.edu; franck.dayan@colostate.edu; todd.gaines@colostate.edu.

[2] Bayer AG, Division CropScience, Weed Control Research, 65926 Frankfurt, Germany. Anita.Kuepper@bayer.com, Falco.peter@bayer.com, Simon.schepp@bayer.com,

[3] Weed Control Platform Lead, Bayer CropScience, St Louis, MO 63141, USA. Alejandro.perez-jones@bayer.com.

[4] University of Illinois, Department of Crop Sciences, Urbana, IL 61801, USA. tranel@illinois.edu.

[5] Senior Scientist Consultant, 65835, Liederbach, Germany. Roland.beffa@t-online.de.

Corresponding author: Todd A. Gaines, todd.gaines@colostate.edu

Submission date: November 21, 2024; number of Figures: 6; number of Tables: 1; Word count: 4,567 (excluding methods)

Supplementary data - number of Figures: 15, number of Tables: 6

HIGHLIGHTS

Our study identifies that the *CYP72A1182* gene has a functional role in metabolic herbicide resistance in *Amaranthus palmeri* and is linked to *cis*-regulatory polymorphisms, advancing metabolic resistance understanding in dicots.

ABSTRACT

Evolution of metabolic herbicide resistance is a major issue for weed management. Few genes and regulatory mechanisms have been identified, particularly in dicotyledonous weed species. We identified putative causal genes and regulatory mechanism for tembotrione-resistance in *Amaranthus palmeri*. Cytochrome P450 candidate genes were identified through RNA-seq analysis. We validated their functions using heterologous expression in *S. cerevisae*. Promoters of the candidate P450 genes were analyzed. We performed QTL mapping to identify genomic regions associated with resistance. *CYP72A1182* deactivated tembotrione. This gene had increased expression in other *A. palmeri* populations resistant to multiple herbicides, including tembotrione. Resistant plants exhibited polymorphisms in the promoter of *CYP72A1182*. We identified QTLs linked to herbicide resistance, including one on chromosome 4 approximately 3 Mb away from *CYP72A1182*. *CYP72A1182* is involved in tembotrione resistance in *A. palmeri*. Increased expression of this gene could be due to *cis*-regulation in the promoter, as well as *trans*-regulation from transcription factors. Further studies are in progress to test this hypothesis. The elucidation of regulatory genes is crucial for developing innovative weed management approaches and target-based novel molecules.

Key Words: gene expression regulation, herbicide resistance, hydroxylation, metabolism, monooxygenase, oxidation.

56 **INTRODUCTION**

57 Evolution of herbicide resistance results from the selection pressure imposed by the
58 frequent and consistent use of herbicides over time (Gaines et al. 2020). The emergence and
59 spread of herbicide-resistant weeds poses a major challenge to sustainable agriculture, as they
60 can diminish crop yields and increase the costs associated with weed control (Chauhan 2020;
61 Oerke 2006). Herbicide resistance in plants can be selected through different mechanisms,
62 primarily classified as target-site (TSR) and non-target-site resistance (NTSR) (Gaines et al.
63 2020; Rigon et al. 2020). Between these two groups, NTSR, specifically metabolic resistance, is
64 a critical issue due to the potential interaction of a single metabolic resistance mechanism with
65 herbicides spanning multiple modes of action (Rigon et al. 2020).

66 Plants possess a diverse array of enzymes involved in the detoxification of xenobiotics.
67 Within these enzymes, cytochrome P450 enzymes (P450) play a key role in the initial step of the
68 detoxification process (Rigon et al. 2020). P450s associated with herbicide metabolism have
69 been identified from various crops (Brazier-Hicks et al. 2022; Kato et al. 2020; Pan et al. 2006;
70 Pan et al. 2022; Siminszky et al. 1999) and implicated in evolved herbicide resistance in weeds.
71 Notable examples from weeds include *CYP81A12*, *CYP81A21*, *CYP81A15*, and *CYP81A14* from
72 *Echinochloa phyllopogon* (Dimaano et al. 2020); *CYP81A69* and *CYP81A70* from *Cynodon*
73 *dactylon* (Zheng et al. 2022); *CYP81A10v7* from *Lolium rigidum* (Han et al. 2021) and
74 *CYP77B34* from *Descurainia sophia* (Shen et al. 2022). Nearly all of the identified genes from
75 weeds to date are from grass species (Rigon et al. 2020).

76 *Amaranthus palmeri* (Palmer amaranth) is a highly invasive and troublesome weed that
77 poses a significant threat to agricultural crops and ecosystems. Native to the southwestern United
78 States, this annual dicot weed has become a pervasive problem across North America and

79 globally due to its aggressive growth, adaptability, and resistance to herbicides (Roberts and
80 Florentine 2022; Ward et al. 2013). *A. palmeri* is dioecious, with separate male and female
81 plants, obligate cross-pollination, and high within- and among-population genetic diversity
82 (Gaines et al. 2021; Ward et al. 2013). Populations have evolved resistance to herbicide spanning
83 nine different modes of action, including synthetic auxins (Foster and Steckel 2022; Shyam et al.
84 2022), glufosinate (Priess et al. 2022), and herbicides targeting acetolactate synthase (ALS)
85 (Berger et al. 2016), 5-enolpyruvylshikimate-3-phosphate synthase (EPSPS) (Gaines et al. 2010),
86 protoporphyrinogen oxidase (PPO) (Montgomery et al. 2021), photosystem II (PSII) (Jhala et al.
87 2014), 4-hydroxyphenylpyruvate dioxygenase (HPPD) (Küpper et al. 2018), very long chain
88 fatty acid elongase (VLCFAE) (Hwang et al. 2023), tubulin biosynthesis (González-Torralva and
89 Norsworthy 2021), and.

90 *A. palmeri* has evolved herbicide resistance through two main mechanisms, TSR and
91 NTSR. The most commonly observed cases of resistance involve TSR to ALS- and EPSPS-
92 inhibitors (Gaines et al. 2010; Palmieri et al. 2022). However, there are increasing resistance
93 cases due to metabolic-based mechanisms (Küpper et al. 2018; Shyam et al. 2022), and further
94 analysis is necessary to identify the specific genes involved and their regulation. RNA-seq
95 analysis plays a crucial role in deciphering the genetic basis of herbicide resistance, especially
96 when resistance is a multigenic trait (Gaines et al. 2014; Kohlhase et al. 2019). Additionally,
97 with the availability of complete genomes for weed species (Montgomery et al. 2024), such as *A.*
98 *palmeri*, conducting Quantitative Trait Locus (QTL) mapping experiments becomes a valuable
99 approach for determining the genetic architecture of resistance (Murphy et al. 2021). By
100 combining comprehensive gene expression data obtained from RNA-seq analysis with QTL

101 mapping, researchers can gain valuable insights into the genetic factors underlying resistance and
102 other important characteristics in weeds.

103 This research aimed to identify and functionally validate metabolic genes associated with
104 resistance to tembotrione (an HPPD inhibitor) within a particular population of *A. palmeri*. We
105 subsequently sought to determine whether an identified gene, *CYP72A1182*, was also associated
106 with resistance in other suspected tembotrione-resistant *A. palmeri* populations. The research
107 also sequenced the promoter and ran a QTL analysis to investigate potential regulation of
108 *CYP72A1182*.

109 MATERIALS AND METHODS

110 Plant material for QTL mapping and RNA-seq analysis

111 The resistant (NER) and susceptible (NES) *A. palmeri* populations were collected from
112 fields in Shickley, Nebraska in 2011. NER is resistant to atrazine and the HPPD inhibitors
113 tembotrione, mesotrione, and topramezone (Jhala et al. 2014; Küpper et al. 2018). The enhanced
114 metabolism of tembotrione to hydroxy-tembotrione was identified as the mechanism of herbicide
115 resistance in the NER population (Küpper et al. 2018). To minimize the impact of genetic
116 differences unrelated to metabolic herbicide resistance, QTL mapping and RNA-seq was
117 performed on pseudo-F2 plants generated from controlled pairings of NER and NES parents. The
118 approaches for the generation of the pseudo-F2 plants are in Methods **S1** and Fig. **S1**.

119 RNA-sequencing analysis

120 Descriptions of plant population, herbicide application, plant tissue collection, and library
121 preparation are in Methods **S1**. Raw reads were pre-processed by removal of library adapter
122 sequences, removal of low quality reads, and assessing the quality control using fastp (Chen et

123 al. 2018). Read alignment of the 108 libraries to the available male genome of *A. palmeri* (v1.1,
124 id55760) (Montgomery et al. 2020) was performed using Hisat2.2.1 (Kim et al. 2019). Most of
125 the reads (>77%) aligned concordantly once, while >7% aligned concordantly more than one
126 time and about 14% of reads aligned not concordantly. Mapped reads were assigned to gene
127 features using featureCounts (Liao et al. 2014).

128 **P450 gene sequences and phylogenetic tree**

129 Consensus sequences of the candidate P450 genes were extracted from the transcriptome
130 and aligned to the reference *A. palmeri* genome (Montgomery et al. 2020) to analyze single
131 nucleotide polymorphisms (SNPs). PCR was performed to amplify the coding sequences in four
132 each of sensitive (S) and resistant (R) plants from the pseudo-F2 population that were used for
133 the RNA-seq experiment. cDNA synthesis was performed using ProtoScript® II First Strand
134 cDNA synthesis kit with 1 µg of RNA. Protein sequences from cytochrome P450 known to
135 metabolize herbicides in different plant species were obtained from NCBI. Multiple protein
136 alignment was performed using ClustalO and used for tree construction with Neighbor-joining
137 method using Geneious Prime® 2023.0.1.

138 **Quantitative reverse transcription-PCR (RT-qPCR) validation**

139 NES and NER populations were grown and tembotrione herbicide was applied at 91 g a.i.
140 ha^{-1} as previously described. Four plants of each population were used for gene expression
141 analysis validation. The youngest leaf tissue was collected at 0, 3, 6, and 12 h after herbicide
142 application (HAT) in 2 mL Eppendorf tubes and placed in liquid nitrogen. The tubes were kept at
143 -80 ºC for further analysis. Tissue was ground with 3 mm stainless steel beads in a TissueLyser
144 (Qiagen) with intensity of 30 for 1 min. RNA was isolated using Direct-zol RNA Miniprep from

145 Zymo Research. cDNA synthesis was performed using ProtoScript® II First Strand cDNA
146 synthesis kit using 1 µg of RNA and purified with DNase I.
147 Relative gene expression was analyzed on a T100 Thermal Cycler (BioRad), using
148 SsoAdvanced™ universal SYBR® Green supermix. Reaction mixtures consisted of 10 µL of
149 SsoAdvanced universal SYBR® Green supermix (2×), 2.5 µL of forward and reverse primers at
150 10 µM, and 5 µL of cDNA (1:20 dilution). Thermocycler conditions consisted of an initial step
151 of 30 sec at 95°C followed by 35 cycles of 5s at 94°C and 30 s at 60°C. Melt curve analysis was
152 added using 65°C with 0.5°C increments of 5 s/step.
153 The reference genes used were *18S rRNA* and *Actin7*. These two genes had the best gene
154 stability as assessed by the NormFinder algorithm (Andersen et al. 2004) (Tab. **S1**). Primers for
155 the reference genes were designed based on conserved regions after alignment of *18S*
156 *(FJ669720.1), actin* (HQ656028.1), and *TUB* (XM_010693569.3) from *Beta vulgaris* with the
157 reference genome from *A. palmeri* (CoGe – v1.1, id55760). The candidate genes tested based on
158 RNA-seq results were *CYP72A1182*, *CYP72A1027*, *CYP72A1015*, and *CYP81CJ2*. Another
159 *CYP72A-like* gene, hereafter named as *CYP72A_4286* was used as a cytochrome P450 not
160 associated with herbicide resistance based on RNA-seq data. Primers for candidate genes were
161 designed on regions based on consensus sequences from the transcriptome and Sanger
162 sequencing of the genes and are listed in Tab. **S2**.

163 **Heterologous expression of CYPs**

164 The genes of interest were transformed and expressed in yeast for further investigation of
165 their role in tembotrione metabolism. Coding sequences of the candidate genes were synthesized,
166 optimized for yeast transformation, and inserted in the pUC-WG/ampv vector by GENEWIZ
167 (Azenta Life Sciences). The gene sequences used were *CYP72A1182* allele 1 (GenBank

168 accession number: OR596705) and 2 (OR596706), *CYP72A1027* (OR596707), *CYP72A1015*
169 allele 1 (OR596708) and 2 (OR596709), and *CYP81CJ2* allele 1 (OR596710) and 2
170 (OR596711). As a positive control, the gene *CYP81A9* from corn, known as *Nsf1*, was used. This
171 gene was identified as the major resistance locus in corn for the herbicides nicosulfuron and
172 mesotrione (Williams and Pataky 2008). Restriction sites for BamHI and EcoRI were added to
173 the 5' and 3' ends, respectively. Kozak sequence (AAAAAATCT) was added at the 5' end as a
174 protein translation initiation site. Restriction enzyme reactions were performed to cut the
175 optimized sequence from the vector using 1 μL EcoRI, 1 μL BamHI, 500 ng of the vector, with
176 incubation at 37°C for 2 h. Reaction products were run on 1% agarose gel electrophoresis and
177 the gene band was isolated and purified using a DNA Gel Purification Kit from New England
178 Biolabs®.

179 The pYES2 yeast expression vector was used for recombinant expression. It contains the
180 *URA3* gene for selection in yeast and 2μ origin for high-copy maintenance and GAL1 promoter
181 to express protein (Thermo Fisher Scientific). The ligation reaction was performed using
182 LigaFast™ Rapid DNA Ligation System from Promega. The reaction consisted of 50 ng
183 digested pYES2 plasmid vector, 5 μL 2× Rapid Ligation Buffer, 1 μL T4 DNA ligase (3 Weiss
184 unit/μL), 50 ng of gene, and purified water up to 10 μL. The reaction was incubated overnight at
185 4°C. The product from the reaction was used to transform *E. coli* using the One Shot® TOP 10
186 kit (Invitrogen). The transformed cells were plated with ampicillin (100 μg/mL) and incubated at
187 37°C overnight. Single colonies were selected, and gene insertion was confirmed by colony PCR
188 using high-fidelity PrimerStar HS DNA polymerase. The gene sequence was confirmed by
189 Sanger sequencing. Plasmids were isolated using ZymoPure II Plasmid Miniprep Kit.

190 **Yeast transformation and tembotrione incubation**

191 Yeast transformation protocol is described in Methods **S2**. Single colonies containing
192 empty pYES2 or the candidate CYP genes were incubated in 15 mL 2% raffinose medium and
193 allowed to grow for 2-3 d at 30 °C. Cell density was measured spectrophotometrically until the
194 OD600 in 20 mL of induction medium was 5. The volume was removed and pelleted at 1,500 ×
195 g for 15 min at 4 °C. The cells were resuspended with 1 mL of induction medium containing 2%
196 galactose and inoculated into 20 mL of the same medium. Tembotrione at 1500 µM diluted in
197 EtOH was applied right after the cells were incubated in the induction medium. The yeast cells
198 were incubated at 30°C at 200 rpm. Twenty-four hours after herbicide application, 5 mL of the
199 medium were collected in 15 mL falcon tubes and cells were pelleted at 1,500 × g for 5 min.
200 The supernatant was collected, and cleaned by adding 5 mL of 5% acetic acid acetonitrile +
201 QuEChERS, vortexed for 30 s, and centrifuged for 15 min at 2,000 × g. The supernatant was
202 collected, filtered through a nylon 13 mm by 0.2 µm (Econofltr Nyln, Agilent Technologies),
203 and injected in the LC-MS/MS.

204 **LC-MS/MS protocol**

205 LC-MS/MS system consisted of a Nexera X2 UPLC with 2 LC-30AD pumps, a SIL-30AC
206 MP autosampler, a DGU-20A5 Prominence degasser, a CTO-30A column oven, and SPD-M30A
207 diode array detector coupled to an 8040 quadrupole mass-spectrometer. For tembotrione, the MS
208 was in negative mode with an MRM optimized for 439.1>226.05 and set for 100 ms dwell time
209 with a Q1 pre-bias of 11.0V, a collision energy of 11.0V and a Q3 pre-bias of 14.0V. For
210 hydroxy-tembotrione, the MS was in negative mode with an MRM optimized for 455.1>419.05
211 and set for 100 ms dwell time with a Q1 pre-bias of 11.0V, a collision energy of 11.0V and a Q3
212 pre-bias of 14.0V. The samples were chromatographed on a 100×4.6 mm Phenomenex Kinetex
213 2.6 µm biphenyl column maintained at 40°C. Solvent A consisted of water with 0.1% formic

214 acid and solvent B was acetonitrile with 0.1% formic acid. The solvent program started at 80% B
215 and increased to 100% B in 3.5 min and maintained at 100% for 2 min. The solvent was returned
216 to 80% B and maintained there for 3 min before the next injection. The flow rate was set at 0.4
217 mL/min and samples were analyzed as 1 μL injection volumes.

218 ***CYP72A1182* and *CYP81CJ2* promoter amplification**

219 Pseudo-F2 plants were grown in the greenhouse and the youngest leaf tissue was collected
220 when the plants reached four to five true leaf stage. Tembotrione was applied at 77 g ha^{-1} rate.
221 Five each of R and S plants from a pseudo-F2 population were chosen for promoter
222 amplification. DNA extraction was performed using hexadecyltrimethylammonium bromide
223 (CTAB) method (Doyle and Doyle 1990). DNA quantification was carried out using Nanodrop
224 2000c (Thermo Fisher Scienfitic). Primers were designed by Primer3Plus
225 (https://www.bioinformatics.nl/) using as reference the available draft genome of *A. palmeri*
226 (Montgomery et al. 2020). The primer sequences used are listed in Tab. **S2**. The methods used to
227 amplify the gene promoter are available in Methos **S3**.

228 **Involvement of *CYP72A1182* in different tembotrione-resistant *A. palmeri* populations**

229 Seeds from *A. palmeri* populations were collected from agricultural fields in 2019 in the
230 United States with suspected herbicide resistance to mesotrione and tembotrione. Whole-plant
231 dose response, ^{14}C-tembotrione metabolism, P450 gene expression and gene copy number were
232 evaluated to test the hypothesis that the same candidate P450 gene is involved in the resistance
233 mechanism in these additional populations. The methods are described in Methods **S4**.

234 **Mapping of tembotrione resistance in NER *A. palmeri* population**

235 ***Library preparation and QTL identification***

236 Dose-response and segregation analysis methods are described in Methods **S5**. Plant tissue
237 was collected before herbicide application for DNA extraction from single leaves following a
238 modified CTAB method. DNA samples were assessed for quality using Qubit. Double-digest
239 restriction site-associated DNA sequencing (ddRADseq) libraries were generated with ApeKI
240 and sequenced using NovaSeq S4 with 150 bp paired-end reads (Illumina). The average yield
241 was around 7.4 M reads per library and the mean quality scores were over Q30 for all libraries.
242 The sequencing was performed at the University of Minnesota Genomics Center.

243 The ddRAD-seq libraries were trimmed using trimmomatic v0.36 (Bolger et al. 2014),
244 aligned to the reference male genome of *A. palmeri* (scaffold file - v1.1, id55760) (Montgomery
245 et al. 2020) with Burrows-Wheeler Aligner (Li and Durbin 2009) and variants called using
246 GATK 4.2.0 (Poplin et al. 2018). Samples were computationally binned by shoot fresh mass.
247 The variant sites were separated by SNPs and insertion/indels and hard filter was performed as
248 following for SNPs - QD < 2.0, QUAL < 30.0, SOR > 4.0, FS > 20.0, MQ < 50.0 and
249 insertion/indels QD < 2.0, QUAL < 30.0, FS > 200.0. The variant sites were filtered based on
250 depth (at least five reads) and only variants that were homozygous were selected. R/qtl2 package
251 was used to find QTLs (Broman et al. 2019). The analysis was performed separately for two
252 distinct crosses (A and B) and combined A + B. QTL intervals were calculated using Bayes
253 credible intervals with the function bayes_int(). To determine the threshold for identifying
254 potential QTL, 1000 permutation tests were conducted at a confidence level of 95%. The critical
255 F value obtained from this analysis was used as the criterion to declare putative QTL. The
256 functional analysis of the genes present in QTLs was conducted using DAVID Bioinformatics
257 Resources v6.8 (Sherman et al. 2022). Statistical analysis for all the experiments is described in
258 Methods S6.

RESULTS

Differentially expressed genes (DEGs)

A total of 20,846 genes were analyzed for differential expression out of the initial set of 29,758 genes assigned by featureCounts. Gene-wise dispersion curve was fitted using the DESeq2 model (Fig. **S2**). There was favorable dispersion pattern, with decreasing dispersion as the mean expression levels increased, indicating a good fit of the DESeq2 model to the analyzed data. The principal component analysis (PCA) plot revealed that PCA1 and PCA2 accounted for 35 and 21% of the variation in the data, respectively (Fig. **S3**). PCA1 separated cross A from cross B, while PCA2 exhibited separation of gene clusters based on HAT within each cross. When clustering all 72 analyzed transcriptome samples, two major clusters emerged, with samples from different crosses grouped together, indicating similarities in gene expression response (Fig. **S4**).

Differentially expressed genes (DEGs) were observed in different comparisons. In the contrast comparison of R versus S at constitutive (0 HAT), 6 HAT, and 12 HAT after herbicide application, R had 37, 2, and 9 up-regulated genes and 3, 2, and 4 down-regulated genes, respectively (Fig. **1a**). Among these genes, only two genes were commonly up-regulated (Fig. **1a**). For the analysis of the genes that were responsive to herbicide application for each phenotype, 39, 530, and 106 genes were up-regulated in S and 6, 185, and 160 were up-regulated in R for the comparisons of time 6 vs 0 HAT, 12 vs 0 HAT, and 12 vs 6 HAT, respectively (Fig. **1a**). The heatmap illustrates the expression of DEGs from these comparisons and indicates a separation in clusters of resistant and susceptible plants (Fig. **1a**).

Several genes associated with the detoxification of xenobiotic substances were consistently identified, suggesting an enhanced genetic metabolism in plants with resistance. These genes

282 included four cytochrome P450 genes, four glutathione-S-transferase genes, seven
283 glycosyltransferase genes, a disease resistance protein, and a detoxification 27 gene (Tab. **S3**).
284 Additionally, two MADS-box transcription factors of types 23 and 27 were found to be up-
285 regulated and arise hypothesis of gene regulation in resistant plants. The resistance mechanism in
286 the resistant population was characterized by increased herbicide metabolism including an initial
287 hydroxylation of the tembotrione molecule (Küpper et al. 2018); therefore, among all
288 differentially expressed genes (DEGs), our focus was on the four cytochrome P450 genes that
289 were consistently up-regulated in the R plants. These genes had the genomic IDs
290 MAKER_29886, MAKER_25717, MAKER_10107, and MAKER_25718, and exhibited fold
291 changes of 18.3, 11.8, 6.2, and 5.4, respectively (Fig**. 1b-d** and Tab. **S3**). None of these genes
292 had differential expression at the 6 HAT time point compared to the susceptible plants (Fig. **1c**),
293 and only one gene (MAKER_29886) exhibited a reactivation at the 12 HAT (Fig. **1c**). This
294 indicates that the susceptible plants responded to the herbicide treatment (Fig. **1c**), where an
295 increased transcription of these genes was observed at 6 and 12 HAT. However, the resistant
296 plants constitutively expressed these cytochrome P450 genes at a higher level prior to herbicide
297 treatment.
298 Constitutively expressed P450s, MAKER_25717, MAKER_25718, and MAKER_29886,
299 had significant similarity to *CYP72A219* from *Spinacia oleracea* (NCBI: XM_056843192.1),
300 with identities of 76.2, 74.3, and 76.3% respectively. Similarly, the gene ID MAKER_10107
301 assigned the name *CYP81CJ2* had high similarity (73.3%) to *CYP81E8* from *Chenopodium*
302 *quinoa* (NCBI: XP_021724107.1). Hereafter, the genes MAKER_25717, MAKER_25718,
303 MAKER_29886, and MAKER_10107 will be referred to as *CYP72A1182*, *CYP72A1027*,

304 *CYP72A1015*, and *CYP81CJ2* respectively, based on P450 gene annotation and naming from a
305 recently assembled *A. palmeri* genome (Raiyemo et al. 2024).

306 **SNPs in cytochrome P450 candidate**

307 There were no single nucleotide polymorphisms (SNPs) causing amino acid changes that
308 were consistently different between S or R individuals in the P450 genes. *CYP72A1182* has a
309 coding sequence of 1544 bp and 517 amino acids. *CYP72A1027* has a coding sequence of 1578
310 bp and 526 amino acids. Both R and S phenotypes shared the same two alleles for these genes.
311 *CYP72A1015* has a length of 1394 bp and 464 amino acids. Susceptible plants had a single allele
312 while R plants had the same allele and an additional allele with amino acid substitutions of
313 Thr307Ser, Phe388Leu, and Ile407Val. *CYP72A1182* and *CYP72A1027* are localized on
314 chromosome four and *CYP72A1015* is localized in chromosome 16. *CYP72A1182* shares identity
315 with *CYP72A1015* and *CYP72A1015* of 76.1 and 55.1%, respectively. Two alleles of *CYP81CJ2*
316 were present in both S and R samples. The gene has a length of 1470 bp and 1479 bp in each
317 allele. The short allele has a deletion of 18 bp in position 35, and the longest allele has a deletion
318 of 9 bp in position 37 when aligned to the draft genome. In the available *A. palmeri* genome, this
319 specific region of the gene exhibits a triplication of PPS amino acids, which may be due to
320 incorrect assembly. All cytochrome P450 possess a conserved cluster of proline in the membrane
321 hinge. Similarly, the sequenced cytochrome P450 exhibits this conserved region.

322 In the phylogenetic tree analysis, *CYP72A* genes from *A. palmeri* clustered with
323 *CYP72A31* from *Oryza sativa*, which can metabolize bispyribac-sodium and bensulfuron-methyl
324 (Saika et al. 2014). *CYP81CJ2* clustered with other P450 of family 81 from grasses but with
325 some significant distances between them (Fig. **S5**). This gene has a low identity when aligned
326 with the other P450s. *ApCYP81CJ2* shares identity of 40.5%, 41.0%, and 39% with *ZmCYP81A9*

327 (Genbank: EU955910.1), *LrCYP81A10v7* (Genbank: MK629521.1), and *EpCYP81A12*
328 (Genbank:AB818460.1), respectively, known to metabolize herbicides in grasses (Brazier et al.
329 2002; Brazier-Hicks et al. 2022; Han et al. 2021; Iwakami et al. 2014).

330 **P450 qPCR validation**

331 *CYP72A1182*, *CYP72A1015*, and *CYP72A1015* were upregulated in NER plants at 3, 6,
332 and 12 HAT, respectively (Fig. **S6**). Among the *CYP72A* genes, *CYP72A1182* had a higher up-
333 regulation at 3 and 6 HAT. Additionally, *CYP81CJ2*, located on chromosome 4, had up-
334 regulation specifically at 6 HAT (Fig. **S6**). These observations deviate from those obtained in the
335 RNA-seq analysis, which indicated that these genes are constitutively higher expressed in
336 resistant plants (Fig. **1**). However, this discrepancy arises due to the utilization of the parental
337 populations NES and NER for gene validation, which exhibit significant individual-level
338 variation in their response to tembotrione. Nevertheless, despite the disparity, the consistency of
339 these findings indicates that the up-regulation of these genes in NER plants differs from that in
340 NES plants.

341 ***CYP72A1182* metabolizes tembotrione in yeast**

342 Following a 24 h incubation period with tembotrione, some transformed yeast treatments
343 converted tembotrione into hydroxy-tembotrione. The chromatogram of the empty vector pYES2
344 revealed solely the presence of the parent tembotrione peak at a retention time of 2.9 min (Fig.
345 **2**). Notably, the *Nsf1* gene exhibited a pronounced affinity for tembotrione, producing hydroxy-
346 tembotrione peak at a retention time of 2.7 min and a dihydroxy tembotrione peak at 2.5 min
347 (Fig. **2**). Among all the candidate P450 genes tested, only *CYP72A1182* converted the parent
348 tembotrione into hydroxy-tembotrione. Both alleles of this gene in the WAT11 and WAT21
349 strains metabolized the herbicide. Conversely, *CYP72A1015*, *CYP72A1015*, and *CYP81CJ2* did

350 not exhibit any ability to metabolize tembotrione. Based on these results, it can be concluded that
351 of the candidate P450 genes, only *CYP72A1182* possesses the capacity to recognize the
352 tembotrione molecule and effectively metabolize it.

353 **CYPs promoter analysis**

354 The DNA segment amplified upstream of *CYP81CJ2* was 1,250 base pairs for both the
355 sensitive and resistant plants (Fig. **3**). Pairwise sequence alignment between two samples
356 revealed 100% identity between the promoters of S and R (Fig. **3a** and Notes **S1**). For the
357 promoter of the *CYP72A1182* gene on chromosome four (MAKER-25717), the primers
358 amplified regions ranging from 1991 to 2004 base pairs for S plants and from 1747 to 1768 base
359 pairs for R plants. Pairwise alignment of *CYP72A1182* promoters revealed sequence differences
360 between S and R, with identity of 76.8% (Notes **S1**). Resistant plants had unique insertions, such
361 as a cytosine at position 45 bp, an 8 bp insertion at position 458 bp, an 8 bp insertion at position
362 1247 bp, and a 31 bp insertion at position 1291 bp upstream. Sensitive plants, on the other hand,
363 had unique insertions, including a 13 bp insertion at position 82, a 10 bp insertion at position 309
364 bp, and a 277 bp insertion at position 746 bp upstream of the gene (Fig. **3b** and Notes **S1**).
365 A total of fifteen significant binding-site motifs were identified in the promoter region of
366 *CYP81CJ2*. Interestingly, all motifs were found in both S and R promoters (Fig. **S7**). In the case
367 of the *CYP72A1182* promoter, a total of twenty-five motifs were discovered. Among these, two
368 motifs were specific to the S promoter, two were specific to the R promoter, and twenty-one
369 motifs were shared between S and R (Fig. **S7** and **S8**). Notably, the R promoter exhibited
370 replication of four motifs. Some motifs were identified as a binding site for transcription factors
371 such as MYB88 (AT2G02820), suppressor factor AIF1 (AT3G05800), and abiotic stress-
372 responsive transcription factor DREB (AT1G77200) based on GOMo analysis (Fig. **S8**).

373 Furthermore, the motif GTTATTTAGTAACTTWKYGTD, which serves as a binding site for
374 the MYB gene transcription factor, was triplicated in the R promoter (Fig. **S8**).

375 **Whole-plant dose response, metabolism, and *CYP* expression in different herbicide**
376 **resistant *A. palmeri***

377 Based on the whole-plant dose response (Fig. **S9**), the confirmation of *A. palmeri*
378 populations with suspected tembotrione resistance revealed distinct variations, with resistance
379 index ranging from 2.4 to 7.9 (Tab. **S4** and **S5**). Tembotrione metabolism was assessed in the *A.*
380 *palmeri* populations using ^{14}C herbicide (Fig. **S10**). The method used in the present study was
381 different from the previous study (Küpper et al. 2018), hence, retention times are slightly
382 different. Parental tembotrione had a retention time of 66.9 min and its major metabolites had
383 retention times of 47.3 (M1), 50.1 (M2), 56.3 (M3), 59.0 (M4), and 67.7 min (M5) (Fig. S11 and
384 S12). NER had higher % area peak of hydroxy-tembotrione (M3/M4), the main metabolite
385 associated with herbicide resistance (Küpper et al. 2018), than the sensitive population at 12
386 HAT (Fig **S10**). The other resistant populations were similar to NER, except for WR2019-044
387 and WR2019-273 (Fig. **S10**). The faster hydroxy-tembotrione production in most populations
388 suggests that enhanced metabolism capacity is the main mechanism of HPPD-resistance of these
389 populations. *CYP72A1182* was upregulated in most resistant populations, either before treatment
390 or 6 HAT (Fig. **S1**). The populations WR2019-034, -137, -140, -199, and -274 had a
391 significantly higher relative *CYP72A1182* expression compared to the sensitive population,
392 ranging from 100 to 658-fold increase. In contrast, the expression of *CYP81CJ2* was not
393 constitutively higher or responsive to tembotrione treatment in *A. palmeri* populations, except in
394 WR2019-140 (Fig. **S1**). The gene copy number of *CYP72A1182* was similar across all resistant
395 populations and with that of sensitive plants (Fig. **S14**). The higher gene expression of

396 *CYP72A1182*, constitutively and after tembotrione application in resistant plants, suggests a
397 crucial role in herbicide resistance in the newly characterized tembotrione-resistant populations.

398 **Degree of dominance and QTL identification**

399 The ED_{50} of NES and NER were 7.9 and 37.3 g, respectively (Tab. **1**), lower than
400 previously reported for these populations (Küpper et al. 2018). However, the resistance index
401 (RI) between these two populations was similar, 4 compared with 3.3 from the previous study
402 (Küpper et al. 2018). Both F1 populations were intermediate between NES and NER in response
403 to tembotrione (Fig. **4**). The degree of dominance was calculated and indicated a co-dominant or
404 semi-dominant trait (cross A = 0.42 and cross B = 0.67) based on the formula proposed by
405 Bourguet and Raymond (1998). Pseudo-F2 populations, resulting from the cross between A and
406 B, exhibited survival rates of 11.4% and 8.8%, respectively. These survival rates are similar to
407 the parental homozygous line NER (12.4%), which was cultivated alongside the pseudo-F2
408 plants.

409 Frequency distribution of fresh weight after herbicide treatment on pseudo-F2 plants had
410 two distinct peaks for each cross, with one peak each indicating phenotypic similarity with each
411 parental population. A normal distribution of R plants had higher biomass (red bars) and the
412 same was identified for S samples (Fig. **5a**). The variant calling analysis identified over 3.4
413 million SNP sites in the *A. palmeri* genome. After filtering, a total of 4,404 SNP variants were
414 detected throughout the entire *A. palmeri* genome. Genome scanning in cross A did not detect
415 any QTLs surpassing the LOD threshold of 6.4 after conducting a permutation test. However,
416 when examining pseudo-F2 plants from cross B, significant QTLs with high effects were found
417 in multiple scaffolds exceeding the LOD threshold of 6.7. The scaffolds include scaffold 10 with
418 LOD of 11.6, scaffold 81 with LOD of 10.1, scaffold 6 with LOD of 9.5, and scaffold 14 with

419 LOD of 8. Each QTL was accompanied by other significant QTLs nearby (Fig. **5b**, Tab. **S6**). For
420 instance, in scaffold 10, there were three QTL peaks. The biggest peak had a LOD score of 11.6
421 at position 11,877,263, and two others peaks had LOD scores of 8.4 and 7.9 at positions
422 10,336,852 and 10,337,656, respectively. The same happened in scaffolds 81, 6, and 14 with
423 nearby peaks. Combining the datasets from cross A and cross B increased the sample size and
424 enhanced the statistical power for the analysis. As a result, the genome scan revealed a more
425 robust QTL effect on scaffold 10, precisely at the same genomic location 11,877,263. The QTL
426 exhibited a higher LOD score of 12.2, indicating a stronger and more significant association with
427 the resistance trait (Tab. **S6**). Additional QTLs were found on scaffolds 6, and 14, but with lower
428 effects.

429 QTL located in scaffold 10 accounted for 23% of the phenotypic variation observed in the
430 data for cross B. Additionally, the QTLs in scaffold 81, 6, and 14 explained 20, 19, and 16% of
431 the phenotypic variation, respectively. However, when the data from both cross A and cross B
432 were combined, the overall phenotypic variation explained by the QTLs slightly decreased. This
433 can be attributed to the absence of any QTL in cross A. Specifically, for the combined data, the
434 QTL in scaffold 10 explained 15% of the phenotypic variation, while the QTLs in scaffold 6 and
435 14 accounted for 10% each (Tab. **S6**).

436 To conduct further analysis, functional annotation was performed on the combined dataset
437 due to its larger number of genes and sample size. The QTLs found in scaffolds 10, 6, and 14 are
438 localized on chromosomes four, eight, and fifteen of *A. palmeri*, respectively, and encompass 82,
439 196, and 25 genes, respectively (Supplemental Information Tab. **S6**). The QTL on scaffold
440 10/chromosome 4 does not contain the *CYP72A1182* gene but is located 3 Mb away. Functional
441 annotation of genes in this QTL indicates a predominant molecular function of protein binding

442 (GO:0005515), RNA binding (GO:0003723), and mRNA binding (GO:0003729), consistent with
443 proteins involved in regulating other proteins or molecules through selective protein interactions
444 (Hudson and Ortlund 2014) (Fig. **S15**). The important TFs that were identified include *DREB2A*,
445 *WRKY* and GATA16 within the QTLs. The QTLs also include nine zinc finger proteins, four
446 ubiquitin proteases, three F-box proteins, three ABC transporters, and three cytochrome P450
447 enzymes.

448 For each QTL, multiple markers were identified. In the case of the QTL in scaffold 10, a
449 total of 54 markers were found, while for the QTL in scaffold 6, 94 markers were identified.
450 However, for the QTL in scaffold 14, only a single marker was detected within a 1 Mb range
451 upstream and downstream of the QTL region. The markers associated with scaffolds 10 and 6
452 displayed a consistent pattern with the evaluated phenotype, where the RR genotype exhibited
453 higher biomasses, while the SS genotype had lower biomasses (Fig**. 6**). In contrast, the single
454 marker found in scaffold 14 did not demonstrate the same consistency as the markers identified
455 in the other QTLs (Fig**. 6i**).

456 **DISCUSSION**

457 The evolution of metabolic herbicide resistance mechanisms in weeds represents a
458 significant challenge in weed control practices (Rigon et al. 2020). These mechanisms enable
459 weeds to metabolize a diverse array of herbicides from various chemical families. Identifying the
460 genes responsible for metabolic resistance and comprehending their regulation holds immense
461 potential for developing improved herbicides and mitigating herbicide resistance. In our current
462 investigation, four consistently up-regulated P450 genes were identified in HPPD-inhibitor
463 resistant *A. palmeri*. These four genes did not have any polymorphisms in the coding sequences
464 between R and S plants. Among these genes, only one, named *CYP72A1182*, deactivated the

465 herbicide tembotrione when tested in a heterologous system. Furthermore, our study revealed
466 that this specific gene is upregulated in other HPPD-inhibitor resistant *A. palmeri* populations
467 collected from various fields across the US, supporting its involvement in conferring herbicide
468 resistance in this globally significant species.

469 In the past, metabolic herbicide resistance in dicot weeds was relatively uncommon, with
470 most documented cases of metabolic resistance and identified P450 genes occurring in
471 monocots. However, recent studies have reported instances of metabolic resistance in dicots such
472 as *A. tuberculatus* in 2017 (Kaundun et al. 2017), *A. palmeri* (Küpper et al. 2018) in 2018, and
473 *Raphanus raphanistrum* in 2020 (Lu et al. 2019). These weed species exhibited resistance to
474 HPPD inhibitors. Metabolic resistance to 2,4-D was identified in *A. tuberculatus* (de Figueiredo
475 et al. 2022) . The identification of P450 genes capable of metabolizing herbicides in dicots is
476 relatively limited. For example, *DsCYP77B34* from *Descurainia sophia*, a broadleaf weed found
477 in Asian wheat fields, conferred resistance to ALS-, PPO-, VLCFA-, and PSII-inhibitors when
478 expressed in *Arabidopsis thaliana* (Shen et al. 2022). Arabidopsis lines expressing *R.*
479 *raphanistrum* genes *RrCYP704C1* or *RrCYP709B1* were resistant to HPPD-inhibitors such as
480 mesotrione *(RrCYP704C1)*, tembotrione *(RrCYP709B1)*, and isoxaflutole *(RrCYP709B1)* (Lu et
481 al. 2023). In *A. palmeri*, *CYP81CJ2* was reported as the primary gene responsible for metabolic
482 resistance in an HPPD-inhibitor resistant population from Kansas, USA (KCTR) (Aarthy et al.
483 2022). The population in that study exhibited enhanced metabolism of tembotrione, and
484 *CYP81CJ2* expression, measured by qPCR, was implicated as the likely cause of tembotrione
485 resistance. However, our study indicates that although *CYP81CJ2* is up-regulated, it is not the
486 causal gene for tembotrione resistance in the NER population. Instead, we have identified
487 *CYP72A1182* as a gene capable of converting tembotrione to hydroxy-tembotrione. This finding

488 represents the first study which mechanistically validated a gene responsible for herbicide
489 metabolism in *A. palmeri*. Given the complex genetic structure indicated by our QTL mapping
490 study, additional genes may be functionally involved in conferring metabolic resistance to
491 tembotrione and this question will be the subject of future research.

492 *CYP81E* has been hypothesized as the gene responsible for 2,4-D metabolic resistance in
493 *A. tuberculatus* (Giacomini et al. 2020). This specific cytochrome P450 gene co-segregated with
494 2,4-D resistance based on RNA-seq analysis conducted on F2 individuals. However, the gene did
495 not co-segregate with HPPD resistance, indicating that the genetic association was specific to
496 2,4-D resistance. Mechanistic gene validation for function in 2,4-D metabolism was not
497 performed (Giacomini et al. 2020). Interestingly, *CYP81E8* and *CYP81CJ2* alleles from *A.*
498 *tuberculatus* and *A. palmeri*, respectively, exhibit high sequence similarity, greater than 92%. A
499 similar behavior of *CYP81CJ2* was observed in this study, with higher expression levels in
500 resistant plants of *A. palmeri*; however, when tested in a heterologous system, this gene did not
501 inactivate tembotrione. Based on this finding, we hypothesized that the NER population might
502 have resistance to 2,4-D due to up-regulation of *CYP81CJ2*. The NER population had a
503 resistance index ranging from 2 to 2.5, but complete control was achieved when 500 a.e. g ha^{-1} of
504 2,4-D was applied (data not shown). This suggests that the NER population may indeed be
505 evolving resistance to 2,4-D; however, resistance to tembotrione is not attributed to *CYP81CJ2*,
506 but rather to *CYP72A1182*.

507 Previous research has highlighted *CYP72A219* as a gene involved in herbicide resistance in
508 weeds. A study indicated that among other metabolic genes, *CYP72A219* had constitutive up-
509 regulation in glufosinate-resistant *A. palmeri* plants, with eight times higher expression levels in
510 resistant plants; however, the study did not perform functional gene validation (Salas-Perez et al.

511 2018). Furthermore, *BsCYP72A219*, along with *BsCYP81Q32* from *Beckmannia syzigachne*,
512 were up-regulated in mesosulfuron-methyl-resistant plants (Wang et al. 2023). These genes were
513 validated in transgenic rice, where only *CYP81Q32* conferred resistance to ALS-inhibitors.
514 Notably, up-regulation of two genes with only one gene having validated metabolic function for
515 herbicide resistance, resembled the observed pattern in the present study. Additionally, an
516 alignment of *CYP81CJ2* from *A. palmeri* revealed a 92.7% identity with *CYP81Q32-like* from
517 *Amaranthus tricolor* (XP_057543510.1), a recently sequenced *Amaranthus* species (Wang et al.
518 2022). This finding indicates a very close relationship between *CYP81CJ2* and *CYP81Q32* and
519 may even represent the same gene, designated with different names. The pattern of co-
520 segregation and up-regulation of these genes in different weed species suggests the presence of
521 common *cis* or *trans*-elements that potentially regulate expression of multiple P450 genes in
522 resistant plants.
523 Distinct promoter sequences for *CYP72A1182* were found in R pseudo-F2 plants compared
524 to S, while no such variations were observed for *CYP81CJ2*. QTLs with high effects on the
525 herbicide resistance trait, localized in chromosomes four, eight, and fifteen were also identified.
526 These QTLs include three cytochrome P450 genes and ABC transporters. While these are
527 important genes and warrant further analysis, a gene responsible for metabolizing tembotrione
528 was identified through RNA-seq analysis and validated, suggesting that the new P450s in the
529 QTL mapping may have a small effect for the resistance mechanism of the NER population. The
530 key findings from the QTL are the diverse set of regulatory genes, including key transcription
531 factors that could play a crucial role in the up-regulation of *CYP72A1182* in resistant plants.
532 Transcription factors such as *DREB2A*, *WRKY,* and *GATA16*, along with zinc finger family
533 found in the mapping analysis are known for their involvement in abiotic stress responses

534 (Banerjee and Roychoudhury 2015; Seale 2020; Zhang et al. 2015). Significantly, it should be
535 highlighted that the identified QTL on chromosome four is located two to three Mbp upstream of
536 the *CYP72A1182* gene. This proximity might suggest that the transcription factor (TF) within the
537 QTL region may regulate the gene, potentially influencing its expression. This regulatory effect
538 could be particularly relevant due to the presence of a distinct promoter sequence observed in
539 resistant plants.

540 Promoters of P450s have been investigated in other weed species. Nucleotide
541 polymorphisms were observed in the promoters of *CYP81A12* and *CYP81A21* in the R alleles of
542 multiple herbicide resistant *Echinochloa phyllopogon* plants; however, these single nucleotide
543 polymorphisms did not exhibit a significant association with herbicide resistance (Iwakami et al.
544 2014). Three SNPs were identified in the promoter region of *BsCYP81Q32* in *B. syzigachne*
545 between the R and S variants, spanning approximately 567 to 1207 base pairs upstream of the
546 gene. These SNPs were responsible for increased expression of *GUS* in tobacco leaves
547 transformed with the gene, suggesting the presence of a crucial sequence within that specific
548 region (Wang et al. 2023). Additionally, the researchers identified a transcription factor,
549 *BsTGAL6*, belonging to the bZIP family, which demonstrated efficient binding to the promoter
550 of *BsCYP81Q32* (Wang et al. 2023). This finding suggests the involvement of a *trans*-element
551 that regulates the expression of *BsCYP81Q32* in resistant plants.

552 Our study successfully identified and validated the metabolic resistant gene, *CYP72A1182*,
553 in the tembotrione-resistant *Amaranthus palmeri* population NER. This gene demonstrated the
554 ability to metabolize tembotrione into the main metabolite hydroxy-tembotrione. We have
555 evidence that this gene is highly upregulated in various *A. palmeri* populations across the United
556 States, which poses a potential threat to weed management strategies targeting this species. We

557 also discovered important QTLs associated with the resistance trait, warranting further
558 investigation and validation for the *CYP72A1182* regulation. Future research focusing on
559 validating the identified transcription factors will shed light on the regulation of P450 genes and
560 enhance our understanding of their regulation in weed species.
561

562 **ACKNOWLEDGEMENTS**

563 This work was supported by funding from the Weed Resistance Competence Center at
564 Bayer AG and USDA National Institute of Food and Agriculture, Hatch projects COL00783 and
565 COL00785 to the Colorado State University Agricultural Experiment Station.

566 **AUTHOR CONTRIBUTIONS**

567 CAGR, AK, AP-J, PJT, RB, FED, and TAG designed the research. CAGR, AK, CS, FP,
568 and SS performed experiments. AK, AP-J, PJT and RB contributed experimental materials.
569 CAGR, FP, SS, and JM analyzed the data. CAGR, FED, and TAG wrote the paper. All authors
570 contributed to editing and approving the paper.
571

572 **CONFLICT OF INTEREST**

573 The authors have no conflicts of interest to declare.

574 **DATA AVAILABILITY**

575 The transcriptome and genome sequencing data that support the findings of this study are
576 available at https://www.ncbi.nlm.nih.gov, with reference numbers GSE243128 and
577 PRJNA1012341, respectively. The gene sequences are available at Genbank accession numbers
578 OR596705- OR596711.

579

580 **Tab. 1**. Logistic equation parameters and resistance index (RI) for survival (% of untreated
581 control) in parental *Amaranthus palmeri* herbicide-susceptible (NES), herbicide-resistant (NER),
582 F1 cross A, and F1 cross B populations in response to tembotrione.

Population	b	ED_{50}				RI	p-value
		Dose ($g\ ha^{-1}$)	Lower CI (95%)	Upper CI (95%)	SE		
NES	2.4	9.3	7.9	10.6	0.7	-	
NER	2.1	37.3	31.2	43.4	3.1	4	<0.001
F1 cross A	2.4	16.6	14.2	19.1	1.2	1.8	0.2
F1 cross B	2.6	23.6	20.15	27	1.7	2.5	<0.001

583 b: slope; ED_{50}: herbicide dose that causes a 50% reduction in plant survival; CI: confidence
584 interval of parameter ED_{50} ($\alpha = 0.05$); RI: resistance index = ED_{50} ratio between populations
585 with NES.
586

587

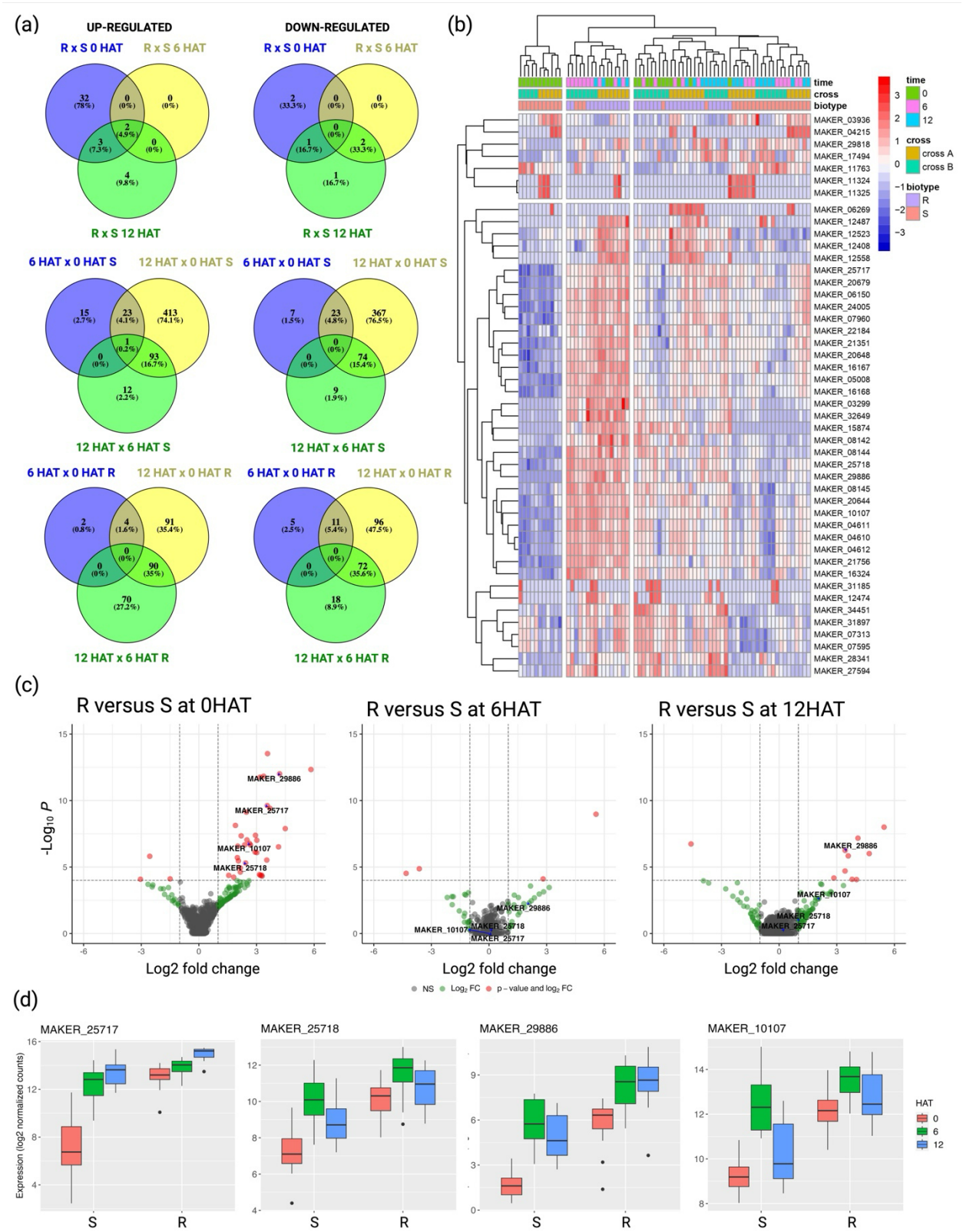

Fig. 1. Analysis of differentially expressed genes (DEGs) in Pseudo-F2 *Amaranthus palmeri*

susceptible (S) and HPPD-resistant (R). (a) The Venn diagram of the up- and down-regulated DEGs indicating unique and common DEGs for 18 different comparisons. (b) Heatmap of top DEGs for the comparisons R vs S at 0, 6 and 12 h after herbicide treatment (HAT). (c) Volcano plots displaying gene expression differences between *Amaranthus palmeri* and treatments of contrast of R versus S before herbicide application (0 HAT), contrast of R versus S at 6 HAT, and contrast of R versus S at 12 HAT. Differentially expressed genes with significant thresholds of p-value <0.0001, adjusted p-value <0.05, log2 fold-change >1 or < -1 are represented by red circles. Dashed lines represent significance thresholds of adjusted p-value<0.05 and log2 fold-change >1 or < -1. (d) The log2 normalized counts of top four cytochrome P450 genes in response to tembotrione in S and R population, MAKER_25717 (*CYP72A1182*), MAKER_25718 (*CYP72A1027*), MAKER_29886 (*CYP72A1015*), and MAKER_10107 (*CYP81CJ2*). Differently expressed genes had a threshold of adjusted p-value of 0.05 and log2 fold-change 1.

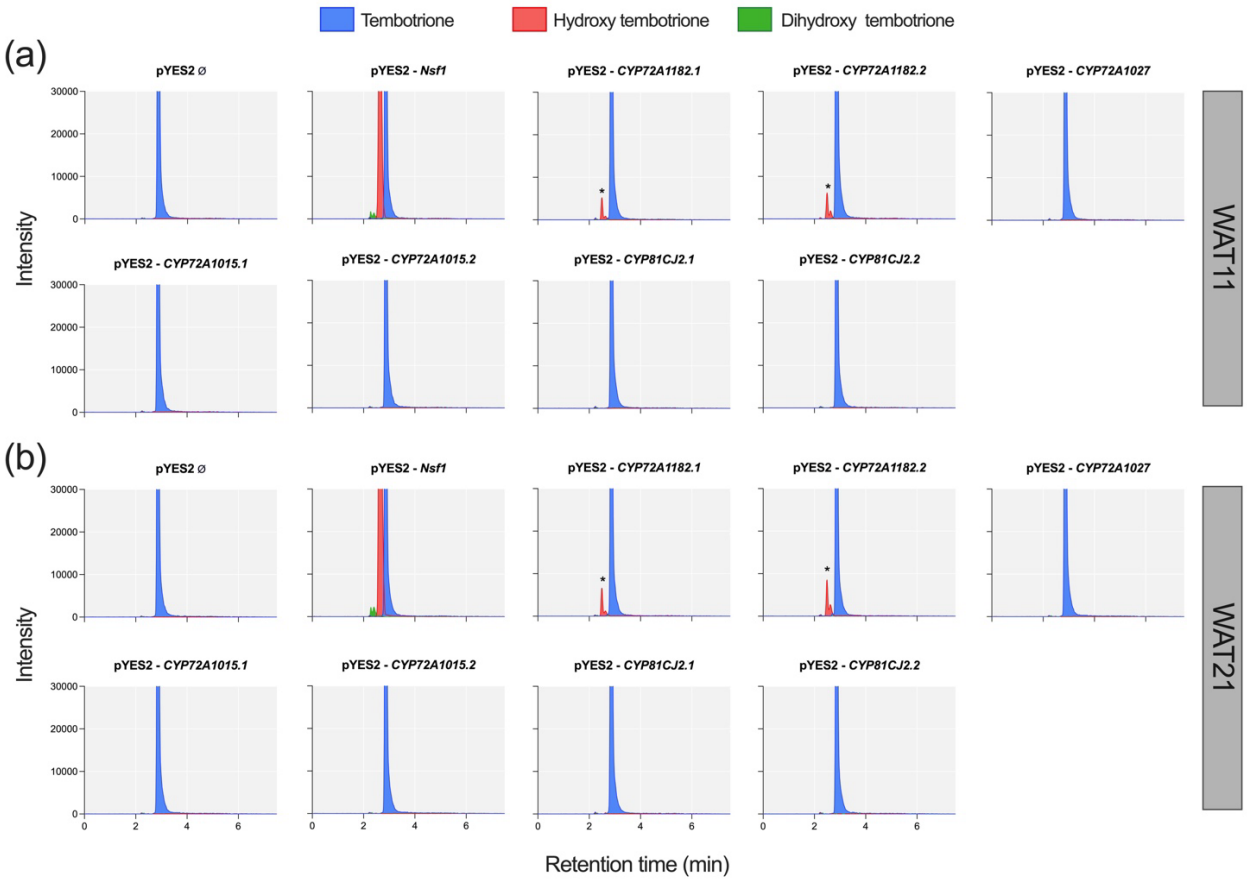

Fig. 2. LC-MS/MS chromatogram of metabolites formed in yeast transformed with P450 genes from *A. palmeri*. Blue peak – parental tembotrione, read peak – hydroxy-tembotrione, green peak, dihydroxy-tembotrione. (a) WAT11 and (b) WAT21 yeast strain carrying *Arabidopsis thaliana* cytochrome P450 reductase 1 and 2, respectively. * at least 10-fold higher peak than the background signal.

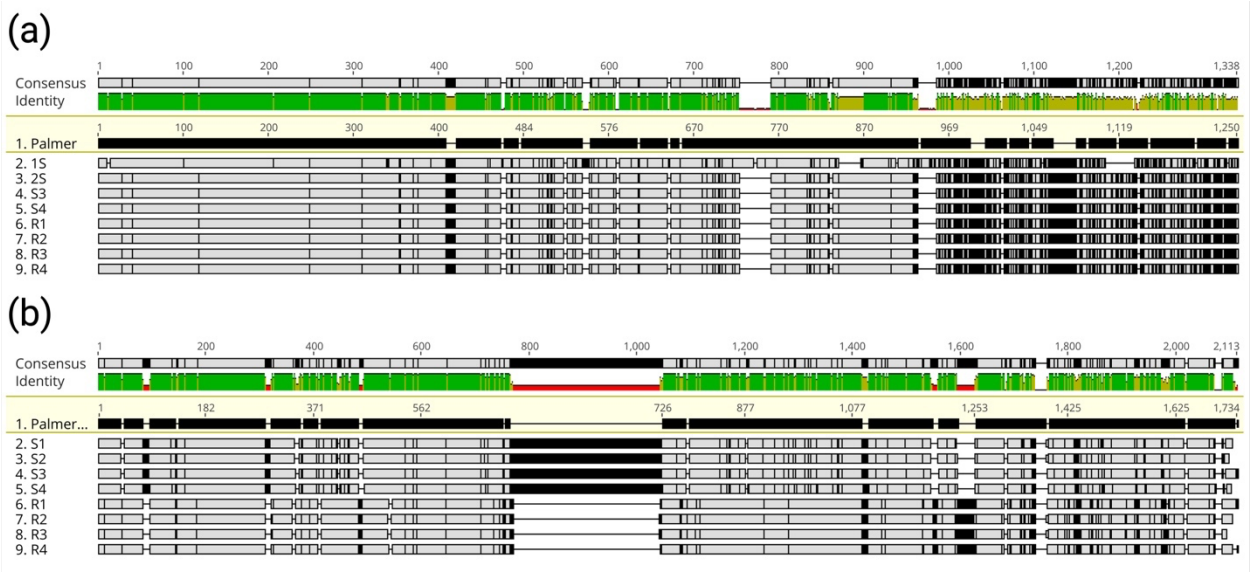

Fig. 3. MUSCLE v5 multiple alignment of *CYP81CJ2* (a) and *CYP72A1182* (b) promoter sequences. The promoter sequences were reverse-oriented from the reference genome sequence to enable viewing in + strand orientation. Black space indicates differences from the reference *A. palmeri* genome (id 55760).

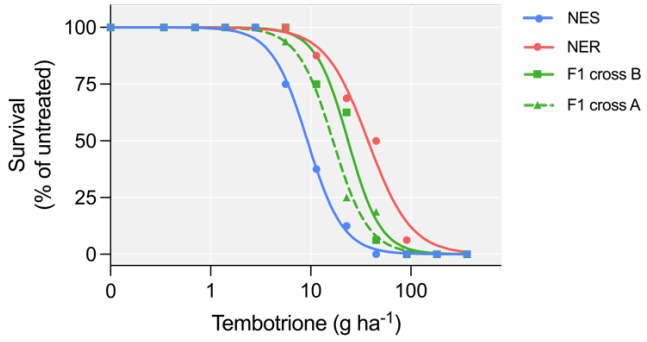

Fig. 4. Dose-response of *Amaranthus palmeri* herbicide susceptible (NES), resistant (NER), F1 cross A and F1 cross B plants in response to tembotrione.

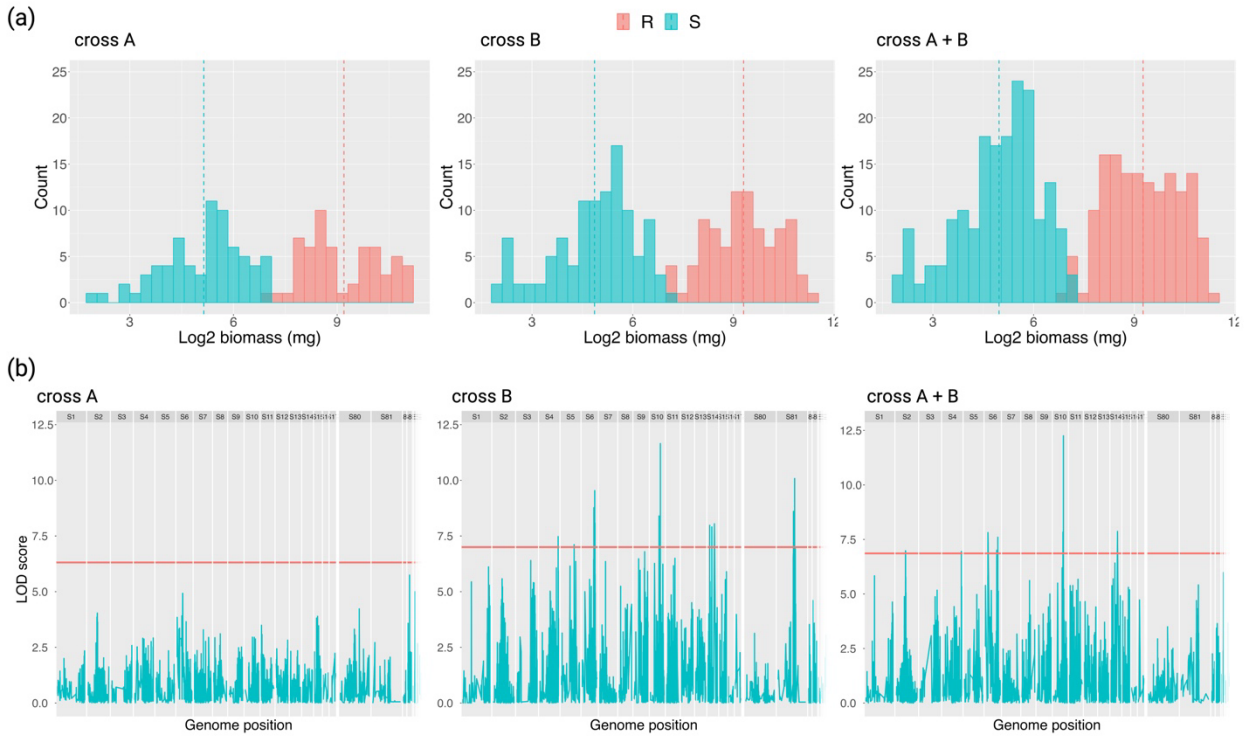

Fig. 5. Frequency distribution and genome scan analysis. (a) Distribution of fresh biomass in plants used for QTL mapping of pseudo-F2 populations from cross A, B, and combined A+B. Blue and red colors represent sensitive and resistant pseudo-F2 plants, respectively. Dashed line indicates the average biomass for parental NES (blue) and parental NER (red). (b) Genome scan of pseudo-F2 *A. palmeri* populations from cross A, B, and combined A+B. y-axis indicates LOD score (logarithm of the odds) statistical estimate, x-axis indicates genome position on scaffolds levels. The plants were treated with 77g ha^{-1} of tembotrione, and fresh biomass was measured after 28 d.

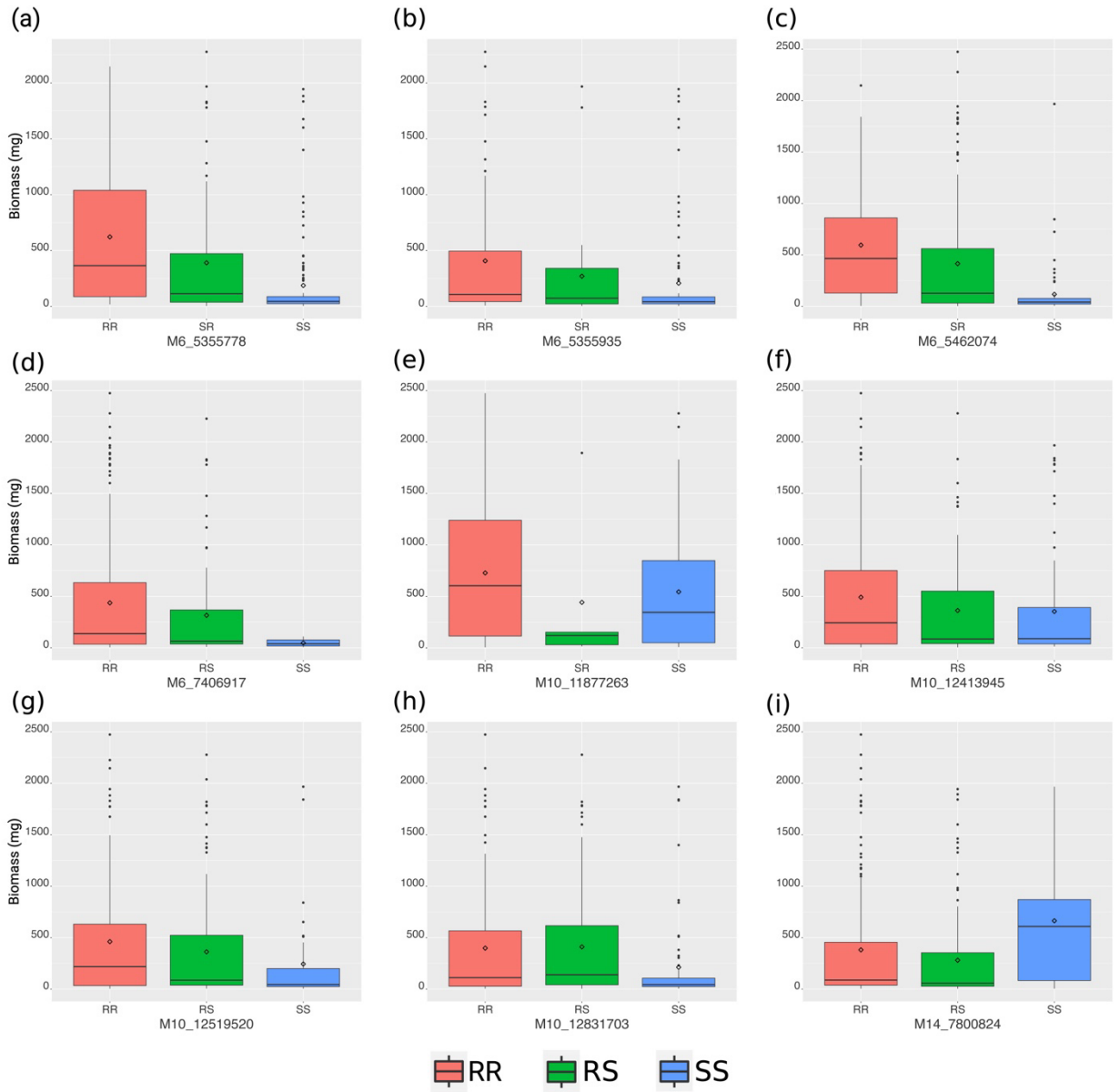

Fig. 6. Markers and resistance phenotypes associated with QTLs for tembotrione resistance in *A. palmeri*. (a) – (d) Markers corresponding to the QTL in scaffold 6 (M6). (e) – (h) Markers corresponding to the QTL in scaffold 10 (M10). (i) Marker in scaffold 14 (M14). Boxplots represent the range of biomass values after herbicide treatment, including the maximum and minimum values, lower and upper quartiles, and the median. The diamond-shaped symbols indicate the average biomass for each genotype.

REFERENCES

Aarthy T., C. Shyam, and M. Jugulam. (2022) Rapid metabolism and increased expression of *CYP81E8* gene confer high level of resistance to tembotrione in a multiple-resistant Palmer amaranth (*Amaranthus palmeri* S. Watson). Frontiers in Agronomy 4, 1010292.

Andersen C. L., J. L. Jensen, and T. F. Ørntoft. (2004) Normalization of real-time quantitative reverse transcription-PCR data: a model-based variance estimation approach to identify genes suited for normalization, applied to bladder and colon cancer data sets. Cancer Res 64:5245-50.

Banerjee A., and A. Roychoudhury. (2015) WRKY proteins: signaling and regulation of expression during abiotic stress responses. Scientific World Journal 2015:807560.

Berger S., P. T. Madeira, J. Ferrell, L. Gettys, S. Morichetti, J. J. Cantero, and C. Nuñez. (2016) Palmer amaranth (*Amaranthus palmeri*) identification and documentation of ALS-resistance in Argentina. Weed Sci. 64:312-320.

Bolger A. M., M. Lohse, and B. Usadel. (2014) Trimmomatic: a flexible trimmer for Illumina sequence data. Bioinformatics 30:2114-20.

Bourguet D., and M. Raymond. (1998) The molecular basis of dominance relationships: the case of some recent adaptive genes. Journal of Evolutionary Biology 11:103-122.

Brazier M., D. J. Cole, and R. Edwards. (2002) O-glucosyltransferase activities toward phenolic natural products and xenobiotics in wheat and herbicide-resistant and herbicide-susceptible black-grass (*Alopecurus myosuroides*). Phytochemistry 59:149-156.

Brazier-Hicks M., S. Franco-Ortega, P. Watson, B. Rougemont, J. Cohn, R. Dale, T. R. Hawkes, A. Goldberg-Cavalleri, N. Onkokesung, and R. Edwards. (2022) Characterization of cytochrome P450s with key roles in determining herbicide selectivity in maize. ACS Omega.

Broman K. W., D. M. Gatti, P. Simecek, N. A. Furlotte, P. Prins, Ś. Sen, B. S. Yandell, and G. A. Churchill. (2019) R/qtl2: Software for Mapping Quantitative Trait Loci with High-Dimensional Data and Multiparent Populations. Genetics 211:495-502.

Chauhan B. S. (2020) Grand challenges in weed management. Frontiers in Agronomy 1:3.

Chen S., Y. Zhou, Y. Chen, and J. Gu. (2018) fastp: an ultra-fast all-in-one FASTQ preprocessor. Bioinformatics 34:i884-i890.

de Figueiredo M. R. A., H. Barnes, C. M. Boot, A. B. T. B. de Figueiredo, S. J. Nissen, F. E. Dayan, and T. A. Gaines. (2022) Identification of a novel 2,4-D metabolic detoxification pathway in 2,4-D-resistant waterhemp (*Amaranthus tuberculatus*). J. Agric. Food Chem. 70:15380-15389.

Dimaano N. G., T. Yamaguchi, K. Fukunishi, T. Tominaga, and S. Iwakami. (2020) Functional characterization of cytochrome P450 *CYP81A* subfamily to disclose the pattern of cross-resistance in *Echinochloa phyllopogon*. Plant Mol.Biol. 102:403-416.

Doyle J. J., and J. L. Doyle. (1990) Isolation of plant DNA from fresh tissue. Focus 12:13-15.

Foster D. C., and L. E. Steckel. (2022) Confirmation of dicamba-resistant Palmer amaranth in Tennessee. Weed Technol. 36:777-780.

Gaines T. A., S. O. Duke, S. Morran, C. A. G. Rigon, P. J. Tranel, A. Küpper, and F. E. Dayan. (2020) Mechanisms of evolved herbicide resistance. Journal of Biological Chemistry 295:10307–10330.

Gaines T. A., G. T. Slavov, D. Hughes, A. Küpper, C. D. Sparks, J. Oliva, M. M. Vila-Aiub, M. A. Garcia, A. Merotto Jr, and P. Neve. (2021) Investigating the origins and evolution of a glyphosate-resistant weed invasion in South America. Molecular Ecology 30:5360-5372.

Gaines T. A., L. Lorentz, A. Figge, J. Herrmann, F. Maiwald, M.-C. Ott, H. Han, R. Busi, Q. Yu, S. B. Powles, and R. Beffa. (2014) RNA-Seq transcriptome analysis to identify genes involved in metabolism-based diclofop resistance in *Lolium rigidum*. The Plant Journal 78:865-876.

Gaines T. A., W. Zhang, D. Wang, B. Bukun, S. T. Chisholm, D. L. Shaner, S. J. Nissen, W. L. Patzoldt, P. J. Tranel, A. S. Culpepper, T. L. Grey, T. M. Webster, W. K. Vencill, R. D. Sammons, J. Jiang, C. Preston, J. E. Leach, and P. Westra. (2010) Gene amplification confers glyphosate resistance in *Amaranthus palmeri*. Proceedings of the National Academy of Sciences, USA 107:1029-1034.

Giacomini D. A., E. L. Patterson, A. Küpper, R. Beffa, T. A. Gaines, and P. J. Tranel. (2020) Co-expression clusters and allele-specific expression in metabolism-based herbicide resistance. Genome Biol. Evol. 12:2267–2278.

González-Torralva F., and J. K. Norsworthy. (2021) Understanding resistance mechanisms to trifluralin in an Arkansas Palmer amaranth population. Genes 12 1225.

Han H., Q. Yu, R. Beffa, S. González, F. Maiwald, J. Wang, and S. B. Powles. (2021) Cytochrome P450 CYP81A10v7 in *Lolium rigidum* confers metabolic resistance to herbicides across at least five modes of action. Plant J. 105:79-92.

Hudson W. H., and E. A. Ortlund. (2014) The structure, function and evolution of proteins that bind DNA and RNA. Nat Rev Mol Cell Biol 15:749-60.

Hwang J.-I., J. K. Norsworthy, P. Carvalho-Moore, L. T. Barber, T. R. Butts, and J. S. McElroy. (2023) Exploratory analysis on herbicide metabolism and very-long-chain fatty acid production in metolachlor-resistant Palmer amaranth (*Amaranthus palmeri* S. Wats.). J. Agric. Food Chem. 71:6014-6022.

Iwakami S., M. Endo, H. Saika, J. Okuno, N. Nakamura, M. Yokoyama, H. Watanabe, S. Toki, A. Uchino, and T. Inamura. (2014) Cytochrome P450 *CYP81A12* and *CYP81A21* are associated with resistance to two acetolactate synthase inhibitors in *Echinochloa phyllopogon*. Plant Physiol. 165:618-629.

Jhala A. J., L. D. Sandell, N. Rana, G. R. Kruger, and S. Z. Knezevic. (2014) Confirmation and control of triazine and 4-hydroxyphenylpyruvate dioxygenase-inhibiting herbicide-resistant Palmer amaranth (*Amaranthus palmeri*) in Nebraska. Weed Technol. 28:28-38.

Kato S., Y. Yokota, R. Suzuki, Y. Fujisawa, T. Sayama, A. Kaga, T. Anai, K. Komatsu, N. Oki, A. Kikuchi, and M. Ishimoto. (2020) Identification of a cytochrome P450 hydroxylase, *CYP81E22*, as a causative gene for the high sensitivity of soybean to herbicide bentazon. Theoretical and Applied Genetics 133:2105-2115.

Kaundun S. S., S. J. Hutchings, R. P. Dale, A. Howell, J. A. Morris, V. C. Kramer, V. K. Shivrain, and E. McIndoe. (2017) Mechanism of resistance to mesotrione in an *Amaranthus tuberculatus* population from Nebraska, USA. PLoS One 12:22.

Kim D., J. M. Paggi, C. Park, C. Bennett, and S. L. Salzberg. (2019) Graph-based genome alignment and genotyping with HISAT2 and HISAT-genotype. Nature Biotechnology 37:907-915.

Kohlhase D. R., J. A. O'Rourke, M. D. K. Owen, and M. A. Graham. (2019) Using RNA-seq to characterize responses to 4-hydroxyphenylpyruvate dioxygenase (HPPD) inhibitor

herbicide resistance in waterhemp (*Amaranthus tuberculatus*). BMC Plant Biology 19:182.

Küpper A., F. Peter, P. Zollner, L. Lorentz, P. J. Tranel, R. Beffa, and T. A. Gaines. (2018) Tembotrione detoxification in 4-hydroxyphenylpyruvate dioxygenase (HPPD) inhibitor-resistant Palmer amaranth (*Amaranthus palmeri* S. Wats.). Pest Manag. Sci. 74:2325-2334.

Li H., and R. Durbin. (2009) Fast and accurate short read alignment with Burrows–Wheeler transform. Bioinformatics 25:1754-1760.

Liao Y., G. K. Smyth, and W. Shi. (2014) featureCounts: an efficient general purpose program for assigning sequence reads to genomic features. Bioinformatics 30:923-30.

Lu H., Q. Yu, H. Han, M. J. Owen, and S. B. Powles. (2019) Evolution of resistance to HPPD-inhibiting herbicides in a wild radish population via enhanced herbicide metabolism. Pest Manag. Sci. 76:1929-1937.

Lu H., Y. Liu, M. Li, H. Han, F. Zhou, A. Nyporko, Q. Yu, S. Qiang, and S. Powles. (2023) Multiple metabolic enzymes can be involved in cross-resistance to 4-hydroxyphenylpyruvate-dioxygenase-inhibiting herbicides in wild radish. Journal of Agricultural and Food Chemistry 71:9302-9313.

Montgomery J., S. Morran, D. R. MacGregor, J. S. McElroy, P. Neve, C. Neto, M. M. Vila-Aiub, M. V. Sandoval, A. I. Menéndez, J. M. Kreiner, L. Fan, A. L. Caicedo, P. J. Maughan, B. A. B. Martins, J. Mika, A. Collavo, A. Merotto, N. K. Subramanian, M. V. Bagavathiannan, L. Cutti, M. M. Islam, B. S. Gill, R. Cicchillo, R. Gast, N. Soni, T. R. Wright, G. Zastrow-Hayes, G. May, J. M. Malone, D. Sehgal, S. S. Kaundun, R. P. Dale, B. J. Vorster, B. Peters, J. Lerchl, P. J. Tranel, R. Beffa, A. Fournier-Level, M. Jugulam, K. Fengler, V. Llaca, E. L. Patterson, and T. A. Gaines. (2024) Current status of community resources and priorities for weed genomics research. Genome Biol. 25:139.

Montgomery J. S., D. A. Giacomini, and P. J. Tranel. (2021) Molecular confirmation of resistance to PPO inhibitors in *Amaranthus tuberculatus* and *Amaranthus palmeri*, and isolation of the G399A PPO2 substitution in *A. palmeri*. Weed Technol. 35:99-105.

Montgomery J. S., D. Giacomini, B. Waithaka, C. Lanz, B. P. Murphy, R. Campe, J. Lerchl, A. Landes, F. Gatzmann, A. Janssen, R. Antonise, E. Patterson, D. Weigel, and P. J. Tranel. (2020) Draft genomes of *Amaranthus tuberculatus*, *Amaranthus hybridus*, and *Amaranthus palmeri*. Genome Biol. Evol. 12:1988-1993.

Murphy B. P., R. Beffa, and P. J. Tranel. (2021) Genetic architecture underlying HPPD-inhibitor resistance in a Nebraska *Amaranthus tuberculatus* population. Pest Manag. Sci. 77:4884-4891.

Oerke E. C. (2006) Crop losses to pests. Journal of Agricultural Science 144:31-43.

Palmieri V. E., C. E. Alvarez, H. R. Permingeat, and V. E. Perotti. (2022) A122S, A205V, D376E, W574L and S653N substitutions in acetolactate synthase (ALS) from *Amaranthus palmeri* show different functional impacts on herbicide resistance. Pest Manag. Sci. 78:749-757.

Pan G., X. Y. Zhang, K. D. Liu, J. W. Zhang, X. Z. Wu, J. Zhu, and J. M. Tu. (2006) Map-based cloning of a novel rice cytochrome P450 gene CYP81A6 that confers resistance to two different classes of herbicides. Plant Mol. Biol. 61:933-943.

Pan L., Q. Guo, J. Wang, L. Shi, X. Yang, Y. Zhou, Q. Yu, and L. Bai. (2022) CYP81A68 confers metabolic resistance to ALS and ACCase-inhibiting herbicides and its epigenetic regulation in *Echinochloa crus-galli*. Journal of Hazardous Materials 428:128225.

Poplin R., V. Ruano-Rubio, M. A. DePristo, T. J. Fennell, M. O. Carneiro, G. A. V. d. Auwera, D. E. Kling, L. D. Gauthier, A. Levy-Moonshine, D. Roazen, K. Shakir, J. Thibault, S. Chandran, C. Whelan, M. Lek, S. Gabriel, M. J. Daly, B. Neale, D. G. MacArthur, and E. Banks. (2018) Scaling accurate genetic variant discovery to tens of thousands of samples. bioRxiv:201178.

Priess G. L., J. K. Norsworthy, N. Godara, A. Mauromoustakos, T. R. Butts, T. L. Roberts, and T. Barber. (2022) Confirmation of glufosinate-resistant Palmer amaranth and response to other herbicides. Weed Technol. 36:368-372.

Raiyemo D. A., J. Montgomery, L. Cutti, F. Abdollahi, V. Llaca, K. Fengler, A. J. Lopez, S. Morran, C. Saski, D. R. Nelson, E. L. Patterson, T. Gaines, and P. J. Tranel. (2024) Chromosome-level assemblies of *Amaranthus palmeri*, *Amaranthus retroflexus*, and *Amaranthus hybridus* allow for genomic comparisons and identification of a sex-determining region. bioRxiv DOI:10.1101/2024.09.18.613719.

Rigon C. A. G., T. A. Gaines, A. Küpper, and F. E. Dayan. (2020) Metabolism-based herbicide resistance, the major threat among the non-target site resistance mechanisms. Outlooks on Pest Management 31:162-168.

Roberts J., and S. Florentine. (2022) A review of the biology, distribution patterns and management of the invasive species *Amaranthus palmeri* S. Watson (Palmer amaranth): Current and future management challenges. Weed Res. 62:113-122.

Saika H., J. Horita, F. Taguchi-Shiobara, S. Nonaka, A. Nishizawa-Yokoi, S. Iwakami, K. Hori, T. Matsumoto, T. Tanaka, T. Itoh, M. Yano, K. Kaku, T. Shimizu, and S. Toki. (2014) A novel rice cytochrome P450 gene, *CYP72A31*, confers tolerance to acetolactate synthase-inhibiting herbicides in rice and arabidopsis. Plant Physiol. 166:1232-40.

Salas-Perez R. A., C. A. Saski, R. E. Noorai, S. K. Srivastava, A. L. Lawton-Rauh, R. L. Nichols, and N. Roma-Burgos. (2018) RNA-Seq transcriptome analysis of *Amaranthus palmeri* with differential tolerance to glufosinate herbicide. PLOS ONE 13:e0195488.

Seale M. (2020) Hot on the trail of DREB2A protein stability. Plant Physiol. 183:7-8.

Shen J., Q. Yang, L. Hao, L. Zhang, X. Li, and M. Zheng. (2022) The metabolism of a novel cytochrome P450 (*CYP77B34*) in tribenuron-methyl-resistant *Descurainia sophia* L. to herbicides with different mode of actions. Int. J. Mol. Sci. 23:5812.

Sherman B. T., M. Hao, J. Qiu, X. Jiao, M. W. Baseler, H. C. Lane, T. Imamichi, and W. Chang. (2022) DAVID: a web server for functional enrichment analysis and functional annotation of gene lists (2021 update). Nucleic Acids Res 50:216-221.

Shyam C., D. E. Peterson, and M. Jugulam. (2022) Resistance to 2,4-D in Palmer amaranth (*Amaranthus palmeri*) from Kansas is mediated by enhanced metabolism. Weed Sci. 70:390-400.

Siminszky B., F. T. Corbin, E. R. Ward, T. J. Fleischmann, and R. E. Dewey. (1999) Expression of a soybean cytochrome P450 monooxygenase cDNA in yeast and tobacco enhances the metabolism of phenylurea herbicides. Proceedings of the National Academy of Sciences, USA 96:1750-1755.

Wang H., D. Xu, S. Wang, A. Wang, L. Lei, F. Jiang, B. Yang, L. Yuan, R. Chen, Y. Zhang, and W. Fan. (2022) Chromosome-scale *Amaranthus tricolor* genome provides insights into the evolution of the genus *Amaranthus* and the mechanism of betalain biosynthesis. DNA Research 30:1-15.

Wang J., L. Lian, J. Qi, Y. Fang, A. Nyporko, Q. Yu, L. Bai, and L. Pan. (2023) Metabolic resistance to acetolactate synthase inhibitors in *Beckmannia syzigachne*: identification of *CYP81Q32* and its transcription regulation. Plant J. 115:317-334.

Ward S. M., T. M. Webster, and L. E. Steckel. (2013) Palmer amaranth (*Amaranthus palmeri*): a review. Weed Technol. 27:12-27.

Williams M. M., and J. K. Pataky. (2008) Genetic basis of sensitivity in sweet corn to tembotrione. Weed Sci. 56:364-370.

Zhang C., Y. Hou, Q. Hao, H. Chen, L. Chen, S. Yuan, Z. Shan, X. Zhang, Z. Yang, D. Qiu, X. Zhou, and W. Huang. (2015) Genome-wide survey of the soybean GATA transcription factor gene family and expression analysis under low nitrogen stress. PLoS One 10:e0125174.

Zheng T., X. Yu, Y. Sun, Q. Zhang, X. Zhang, M. Tang, C. Lin, and Z. Shen. (2022) Expression of a cytochrome P450 gene from Bermuda grass *Cynodon dactylon* in soybean confers tolerance to multiple herbicides. Plants 11:949.

SUPPORTING INFORMATION

Fig. S1. Scheme of crosses performed to generate Pseudo-F2 generation from *Amaranthus palmeri* population HPPD-resistant (NER) x susceptible (NES).

Fig. S2. Gene-wise dispersion estimates.

Fig. S3. Scatterplot of principal components.

Fig. S4. Distance hierarchical clustering heatmap.

Fig. S5. Phylogenetic analysis.

Fig. S6. Relative gene expression of candidate cytochrome P450 genes in parental NES and NER plants.

Fig. S7. Motifs analysis using MEME-suite tool.

Fig. S8. Motif sequences found in *Amaranthus palmeri CYP72A1182* promoter in sensitive and resistant pseudo-F2 plants.

Fig. S9. Dose response of tembotrione in different *Amaranthus palmeri* populations.

Fig. S10. Parental tembotrione and metabolites in HPPD resistant populations of *Amaranthus palmeri* over time after tembotrione application.

Fig. S11. Chemical structures of tembotrione and the main metabolites.

Fig. S12. Representative reverse-phase HPLC chromatogram for *Amaranthus palmeri*

populations at 48 HAT with ^{14}C-Tembotrione.

Fig. S13. Relative gene expression of candidate cytochrome P450 genes in different *Amaranthus palmeri* populations.

Fig. S14. *CYP72A1182* copy number relative to *ALS* in different populations of *Amaranthus palmeri*.

Fig. S15. Functional enrichment of genes from QTLs of scaffold 10, scaffold 6 and scaffold 14.

Table S1. Gene stability assessed by NormFinder algorithm.

Table S2. Primer sequences used for different experiments and their characteristic.

Table S3. Constitutively differentially expressed genes between tembotrione resistant and susceptible *Amaranthus palmeri*. Adjusted *P*-value <0.01.

Table S4. Logistic equation parameters and the resistance index (RI) of survival (% of untreated control) for different populations of *Amaranthus palmeri* subjected to different doses of tembotrione.

Table S5. Logistic equation parameters and the resistance index (RI) of shoot fresh weight (of untreated control) for different populations of *Amaranthus palmeri* subjected to different doses of tembotrione.

Table S6. Quantitative trait loci found in Pseudo-F2 *Amaranthus palmeri* in cross B and combined cross A + B for the trait of HPPD resistance.

Methods S1 Plant material for QTL mapping and RNAseq experiment

Methods S2. Yeast transformation

Methods S3. Promoter amplification

Methods S4. Involvement of CYP72A1182 in different HPPD-resistant *A. palmeri* populations

Methods S5. Dose-response and segregation analysis

Methods S6. Statistical analysis

Notes S1 Alignment of *CYP81CJ2* and *CYP72A1182* promoter between susceptible and resistant *Amaranthus palmeri*.